

Autonomous frequency stabilization of two extended cavity diode lasers at the potassium wavelength on a sounding rocket

Aline N. Dinkelaker¹, Max Schiemangk¹, Vladimir Schkolnik¹, Andrew Kenyon¹, Kai Lampmann², André Wenzlawski², Patrick Windpassinger², Ortwin Hellmig³, Thijs Wendrich⁴, Ernst M. Rasel⁴, Michele Giunta^{5,6}, Christian Deutsch⁵, Christian Kürbis⁷, Robert Smol⁷, Andreas Wicht^{1,7}, Markus Krutzik¹, Achim Peters^{1,7}

¹ Institut für Physik, Humboldt-Universität zu Berlin, 12489 Berlin, Germany

e-mail: aline.dinkelaker@physik.hu-berlin.de

² Institut für Physik, Johannes Gutenberg-Universität Mainz, 55099 Mainz, Germany

³ Institut für Laserphysik, Universität Hamburg, 22761 Hamburg, Germany

⁴ Institut für Quantenoptik, Leibniz Universität Hannover, 30167 Hannover, Germany

⁵ Menlo Systems GmbH, 82152 Martinsried, Germany

⁶ Max Planck Institut für Quantenoptik, 85748 Garching, Germany

⁷ Ferdinand-Braun-Institut, Leibniz-Institut für Höchstfrequenztechnik, 12489 Berlin, Germany

Abstract We have developed, assembled, and flight-proven a stable, compact, and autonomous extended cavity diode laser (ECDL) system designed for atomic physics experiments in space. To that end, two micro-integrated ECDLs at 766.7 nm were frequency stabilized during a sounding rocket flight by means of frequency modulation spectroscopy (FMS) of ³⁹K and offset locking techniques based on the beat note of the two ECDLs. The frequency stabilization as well as additional hard- and software to test hot redundancy mechanisms were implemented as part of a state-machine, which controlled the experiment completely autonomously throughout the entire flight mission.

1 Introduction

Laser systems are a key technology for space-borne applications in optical communication, time keeping, inertial navigation, and geodesy [1, 2, 3, 4, 5, 6], as well as high precision measurements in fundamental physics, such as clock comparisons [2, 7, 8], gravitational wave detection [9, 10], and cold atom based quantum sensors [11, 12]. The laser system described in this paper is motivated by the developments and demands of cold atom based quantum sensors for tests of the Einstein equivalence principle (EEP) [13, 14, 15] on future satellite missions (e.g. [11, 16]). In this context, laser light is required for optical cooling, trapping, manipulation, and detection of the atoms. This poses high demands on the laser system's functionality, specifically on laser frequency, intensity,

their corresponding stability, and tuning range. Additional requirements on mechanical stability, weight, and size of the hardware arise from the deployment to space itself. Beyond that, redundancy and autonomy features should be implemented due to restricted access to the experiment.

Before reaching out to space, any experiment and its subsystems have to be qualified in terms of technological readiness by means of environmental testing. Additionally, experimental sequences have to be developed and parameters optimized in a scenario that resembles the target environment. In the context of quantum sensors for EEP tests in space, this includes microgravity. On ground, these quantum sensors can be tested in microgravity at a drop tower, e.g. the ZARM Bremen drop tower [17, 18, 19], where microgravity ($< 10^{-6} g$) of several seconds (up to 9.6 s) can be achieved. Airborne tests can be conducted on parabolic flights [15], where longer times (about 20 s per parabola on-board a Novespace A300 Zero- g airplane) of reduced gravity ($< 0.05 g$) are possible. For an environment that is closer to conditions on a satellite or the International Space Station (ISS), sounding rockets are the ideal test bed, providing several minutes in reduced gravity better than $10^{-4} g$. They are also a suitable preparation for a future transport of the experiment to Earth-orbit platforms.

The KALEXUS (German acronym for *Kalium Laser Experimente Unter Schwerelosigkeit*) experiment tests a frequency stabilized semiconductor diode laser system on-board the TEXUS 53 sounding rocket. Semiconductor diode lasers are chosen as light sources as they are compact, robust, and available at a variety of wavelengths. This enables complex systems with a

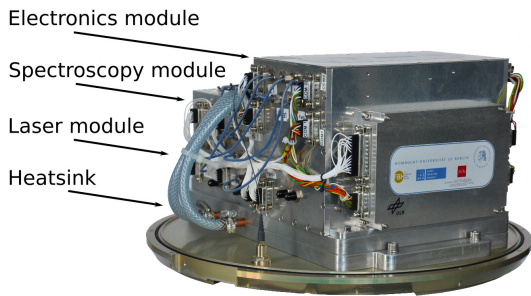


Fig. 1 The KALEXUS payload has a size of $345 \times 218 \times 186 \text{ mm}^3$ ($L \times W \times H$) and a mass of 16 kg. It consists of three different modules integrated into individual, space-grade aluminum housings, connected via optical and electrical interfaces, and mounted onto a heatsink. During flight, the experiment is heat shielded and pressurized within a dome (not shown).

high degree of functionality that fit the tight form factors of space-platforms and withstand harsh environments. With the KALEXUS experiment, we have built a laser system technology demonstrator that incorporates core technologies of a space-based reference laser system for atomic physics experiments. The KALEXUS experiment is based on two narrow linewidth ($< 100 \text{ kHz}$ at $100 \mu\text{s}$ measurement time) extended cavity diode lasers (ECDLs) [20] that emit light at the potassium (^{39}K) D_2 transition wavelength of 766.7 nm . The ECDLs have specifically been designed and built for applications in cold atom experiments on sounding rockets. An absolute frequency stabilization of one laser on the atomic transition of ^{39}K by means of frequency modulation spectroscopy (FMS) [21] is combined with a relative frequency stabilization using a beat note measurement between the two lasers. Hardware tests and flight demonstration of this frequency stabilized laser system are the main goal of the KALEXUS experiment. We combine these hardware tests with two additional features: autonomy and redundancy. Both are specifically important for space applications where experimenters can not easily interact with the experimental setup. We implemented an autonomy concept that automates the steps required to achieve a frequency stabilized laser system for cold atom experiments in a non-laboratory environment. For the redundancy concept, hardware and software architectures are combined to implement backup and switching options that reduce single points of failure. Thus, KALEXUS is a pathfinder experiment for ECDL technology and automated laser stabilization in space. Various applications will benefit from an increased experience and technology readiness level (TRL) [22, 23] of such laser systems.

The overall setup of the KALEXUS experiment and its main subsystems are described in Section 2. An analysis of the experiment performance during the flight is

presented in Section 3. Section 4 gives a summary and outlook.

2 Experimental Setup

The KALEXUS experiment autonomously frequency stabilizes two ECDLs on a sounding rocket using FMS, and the relative frequency difference between the lasers.

Sounding rockets – as other space platforms – have strong requirements regarding the size and the robustness of their payload (for a description of the TEXUS sounding rockets, see e.g. [24, 25, 26]). Due to the limited space inside the rocket, the payload has to be compact and fit inside the available cylindrical volume. It also needs to withstand strong vibrations and accelerations during liftoff, reentry into the atmosphere, and landing. A typical profile of the accelerations during launch of the two-stage VSB-30 rocket motor that is used in the TEXUS sounding rocket program can be found in [27], overall flight duration and altitude are given in [28]. On sounding rockets, the microgravity time available for experiments is generally limited to a few minutes, which means that complete functionality of the experiments needs to be restored quickly after launch.

The KALEXUS setup is designed to fulfill these requirements. It uses a modular architecture consisting of a laser module, a spectroscopy module, and an electronics module. Each module has an individual housing with optical and electrical interfaces. A picture of the assembled flight system is shown in Fig. 1. To counteract temperature increase due to excess heat from the electronics during the flight, a heat sink made from an aluminum block with copper pipes is placed underneath the main experiment modules. Up to several seconds before launch, the heat sink is water cooled to $18 \text{ }^\circ\text{C}$, and provides a limitation of the temperature increase of the laser module to 3 K during the whole flight. The heat sink is mounted to a base plate that fits inside the TEXUS sounding rocket, which confines the experiment diameter to 375 mm . The experiment has a height of 186 mm and a mass of 16 kg . It is enclosed by a pressurized metal dome at 1.2 bar . The system was subject to thermal, pressure, and electrical interface tests, and the hardware was vibration tested at $8.1 g_{RMS}$ to qualify for flight.

The optical layout of the experiment is shown in Figure 2. Fiber coupled light is split off from both lasers and overlapped on a fast photodiode for beat note detection. Light from each laser is also guided to the spectroscopy board via an optical switch. Additionally, light from ECDL 1 bypasses the optical switch and is directly connected to the spectroscopy board, while light from ECDL 2 is split off for external detection.

With the spectroscopy setup, one laser can be frequency stabilized by means of FMS (spectroscopy lock). The second laser is then frequency stabilized with a fixed offset relative to the first one using the beat note fre-

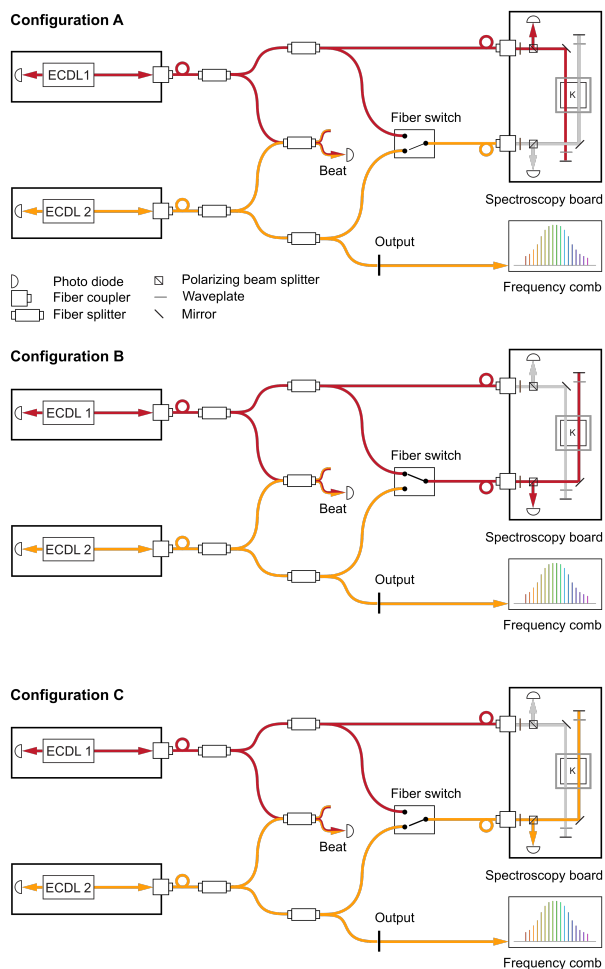


Fig. 2 Schematic of the optical layout: light from two ECDLs is fiber coupled and guided via different paths to the spectroscopy module and the beat note detection. The optical paths can be switched between three different configurations (A, B, C, from top to bottom), so that the path through the spectroscopy module can be changed and the methods of frequency stabilization can be swapped between the lasers. This is part of the implemented redundancy concepts. Light from ECDL 2 also leads out of the KALEXUS dome for external frequency measurements via an optical interface: it is connected to the optical frequency comb by Menlo Systems that is part of the FOKUS experiment [29,30].

quency measurement (offset lock). By using the incorporated redundancy architecture, the frequency stabilization method assignment can be exchanged between ECDL 1 and ECDL 2. The redundancy hardware includes the optical switch, synchronized RF-switches, and a dual spectroscopy setup. In total, three different optical path configurations are possible: configurations A, B and C. An overview is shown in Figure 2 and summarized in Table 1.

In the default configuration (A), light from ECDL 1 that bypasses the optical switch is used for the spectroscopy lock. For the other two configurations, light that enters the spectroscopy board through the opti-

Config.	ECDL 1	ECDL 2	Optical Switch
A	Spectroscopy	Offset	bypassed
B	Spectroscopy	Offset	used
C	Offset	Spectroscopy	used

Table 1 Optical path configurations.

cal switch is used for the spectroscopy lock, either from ECDL 1 (config. B) or from ECDL 2 (config. C). In each configuration, the laser that is not spectroscopy locked is stabilized with an offset lock.

During flight, the experimental control switches between the three beam paths and stabilizes the lasers each time. Stabilization of both lasers as well as tests of this redundancy architecture are performed completely autonomously. The following sections will describe the experiment’s subsystems and the experimental control.

2.1 Laser system

The laser system consists of two micro-integrated ECDLs that emit light at the ^{39}K D₂ transition wavelength of 766.7 nm. ECDLs are often used in ground based precision experiments in which a narrow linewidth and low frequency noise are of advantage, e.g. for phase-locked lasers ([31], see also [32]). In the context of space applications, mechanical stability is an additional, important factor. Here, monolithic diode lasers – distributed feedback (DFB) or distributed Bragg reflector (DBR) – have been favored due to their intrinsic mechanical stability. In addition, the same consortium as involved in the KALEXUS experiment has already carried out successful technology tests with DFB lasers as light sources in drop tower experiments [33] and on sounding rockets [29,30,12]. Since these types of lasers come with a broader linewidth and higher frequency noise compared to ECDLs [34], future scientific experiments would benefit from space-qualified ECDL technology. Recently, compact and robust ECDLs have been developed to enable their use for space applications. The KALEXUS laser system is based on this type of laser, of which a thorough description and characterization can be found in [20].

Each laser has an aluminum nitride micro-optical bench as base plate, on which a ridge-waveguide laser diode, micro-optics, and micro-electronics are integrated, see Figure 3. Light exits from the front and the rear of the laser diode. The extended cavity is formed by the front facet of the laser chip and a volume holographic Bragg grating (VHBG), which is positioned at the rear of the laser module. On the front side of the laser diode and after passing a micro-isolator, the main beam is fiber coupled directly on the micro-optical bench using a Zerodur [35] fiber coupler. The fiber coupling technique is described in [36]. With coupling efficiencies around 65%, we have about 15 mW available ex fiber at maximum

current. A free space photodiode on a circuit board behind the laser module monitors the optical power of the rear beam of each laser. Each laser is temperature stabilized with an individual peltier element for laser body and a micro-thermoelectric cooler for its VHBG, with temperature setpoints near 28 °C. The lasers operate at currents between 150 and 236 mA. However, the exact values depend on the software detection that is part of the automated frequency stabilization.

Before entering the spectroscopy board for frequency stabilization (see Figure 2), the light of the two lasers passes through a fiber based distribution system inside the spectroscopy module, which is shown in Figure 4.

2.2 Spectroscopy

The spectroscopy board itself (see Figure 4) is based on an optical bench made from Zerodur [35] – as described in [36] – with a footprint of $100 \times 75 \text{ mm}^2$ and a thickness of 35 mm. Using the glass ceramic Zerodur as master-material has the advantage of a negligible temperature-induced expansion ($0 \pm 0.02 \times 10^{-6} \text{ K}^{-1}$ [35,36]) over a broad range of temperatures. With monolithic optics and adhesive bonding the setup gains further stability.

Two separate beam paths for saturated absorption spectroscopy are necessary for the redundancy architecture described above. They are realized on the spectroscopy board (Figure 4), as shown schematically in Figure 2. The two paths use separate beam guiding optics, but share one vapor cell for volume optimization. Pump and probe beams for FMS are realized by retro-reflecting the incoming beam behind the vapor cell. To increase the vapor pressure in the cell, it is heated to a temperature of about 40° C. By reading out the photodiode behind the vapor cell, the FMS signal can be used to stabilize the emission frequency of the laser to the $^{39}\text{K } F = 1/2 \rightarrow F'$ crossover line of the D_2 transition.

2.3 Electronics

The electronics module houses an on-board computer (OBC) and the control electronics for the entire experiment, which are shown in Figure 5. A single power source is needed for the experiment during the flight. Voltage conversion and power distribution happens inside the electronics module. The power consumption of the whole KALEXUS system lies around 43 W.

For the control electronics, a modular system of 10 individual cards with specific functionality is combined to form a stack that is connected via a bus system. Each card has a footprint of $100 \times 100 \text{ mm}^2$ and a thickness of around 17 mm. The stack contains cards to control the temperatures and currents of the two ECDLs, count the frequency of the beat note between them, read in several photodiode signals for monitoring, and stabilize the lasers to the spectroscopy signal and the beat note

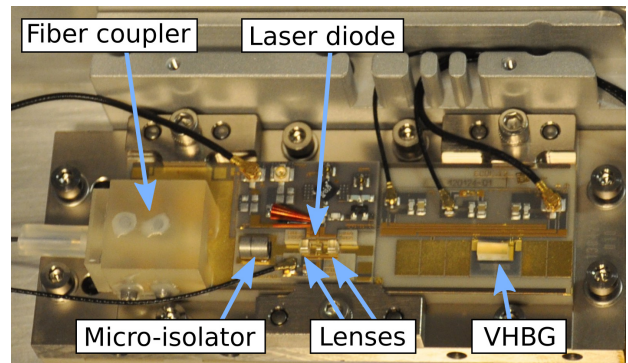


Fig. 3 One of the fiber coupled ECDLs. The microbench has a footprint of $25 \times 80 \text{ mm}^2$. Two ECDLs are inside the laser module (not shown here) with outer dimensions of $145 \times 195 \times 42 \text{ mm}^3$.

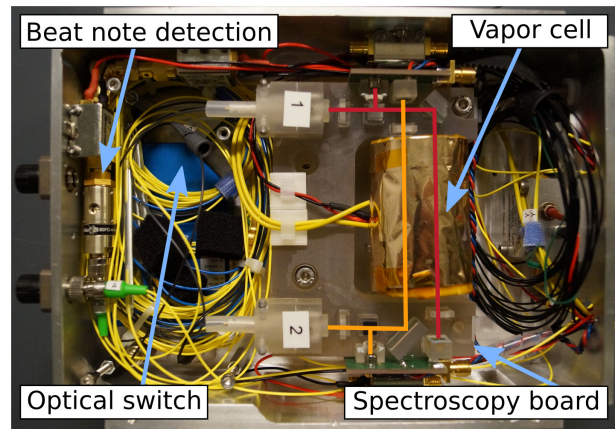


Fig. 4 Spectroscopy module ($145 \times 195 \times 67 \text{ mm}^3$) housing the optical switch, beat note detection, and spectroscopy board. The spectroscopy board consists of a Zerodur optical bench with a heated K vapor cell and an optical setup for FMS.

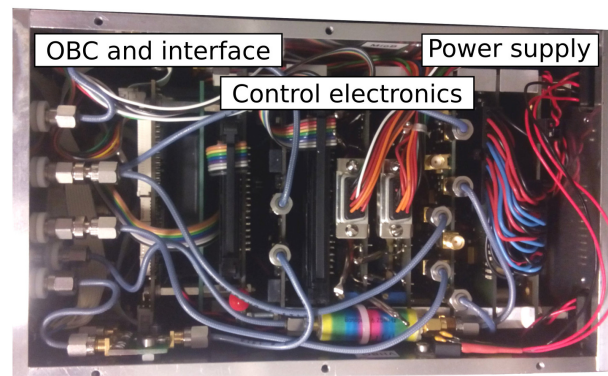


Fig. 5 Electronics module with the on-board computer (left) and the control electronics (right). Included are cards to control the laser currents, laser temperatures, laser frequency and additional cards for detection of photodiode signals, power supply and interface to the OBC. The electronics module has dimensions of $128 \times 218 \times 157 \text{ mm}^3$.

frequency [37]. The complete software for autonomous experiment control runs on the OBC, which is a Kontron MOPSldLX. It is connected to the control electronics and supported by FPGAs on the control electronics for time-critical jobs.

2.4 Experiment control

Experiment control is incorporated in the overlaying structure of a time-dependent experimental sequence. Within the sequence, the software autonomously controls individual hardware components, e.g. through laser current adjustment or optical switching. The experimental sequence is divided into different parts: there are two phases (phase 1 and phase 2) with different experimental objectives during microgravity, as well as additional parts for preparation, launch, reentry and landing, in order to optimize the experiment and to protect the payload from damage. Phase 1 of the experimental sequence in microgravity tests autonomous frequency stabilization and redundancy architecture. Here, the optical path configuration is switched between all three possible options (A, B, C) and frequency stabilization of both lasers is realized each time. In phase 2, the lasers are constantly stabilized in the default configuration, and laser parameters and beat note frequency are monitored. The beat note frequency is also monitored externally through comparison with the FOKUS [29,30] experiment launched on the same rocket. To fall inside the range required for the external frequency comparison, the target value for the offset frequency is kept constant at 464 MHz throughout the flight.

The autonomy concept was implemented in form of a multi-level state-machine. After switch-on, the OBC automatically starts the autonomous control software and enters the experimental sequence. The program uses the first level of the state-machine – the experimental state-machine – to determine when to go from one part in the sequence to the next. On this level, our software reacts to signals that it receives from the TEXUS system. The signals are programmed at specified times relative to liftoff and have been determined using calculated flight parameters, such as microgravity start and end. Figure 6 (top) shows the experimental sequence with the relevant experimental states, illustrating the first level of the state-machine.

Within each state of the experimental sequence, the second level of the state-machine – the locking state-machine – automatically stabilizes the emission frequencies of both lasers using an automated locking mechanism, and evaluates the frequency locks. The automated locking mechanism is applied to both, the spectroscopy and the frequency-offset stabilization. It follows three main steps: first a pattern detection, then a fine-tuning algorithm, and finally onset of the feedback loop. The program starts by stabilizing one laser using the spectroscopy locking technique. For the first step of the laser

stabilization, the current is changed coarsely until the standard deviation of the FMS error signal – normalized for noise – passes a threshold value, which indicates atomic absorption and thus roughly correct frequency. In the second step, the FMS error signal is compared to a stored reference signal. Here, a cross-correlation function is used to determine the frequency offset (algorithm based on [38]). Subsequently, the injection current is adjusted in order to match the two signals. Once the adjustment is complete, i.e. the laser’s frequency scan is centered around the desired absorption peak, the stabilizing feedback loop is activated in the final step. For the offset-frequency stabilization, the same three steps are used, but the input signals and corresponding threshold criteria are different: e.g. for pattern detection, the laser frequency scan has to yield a linear beat note frequency signal with a specific slope. The locking state-machine monitors whether both lasers are stabilized by analyzing the error signals, beat note frequency, and feedback currents. If required, frequency stabilization with the automated locking mechanism is re-initialized automatically.

In order to combine redundancy architecture and autonomy concepts, the selection of redundancy hardware options (i.e. switching optical paths) is incorporated into the software: while in microgravity, the locking state-machine monitors the time it takes to frequency stabilize a laser. If the laser cannot be frequency stabilized within a specified time, the program automatically switches to the next beam path configuration (see Table 1). This way, the time that is potentially lost due to malfunctioning hardware is limited.

Laser monitoring and housekeeping data as well as state-machine information is stored on the OBC flash disk. Every 3 seconds, a reduced data set is sent to ground via a serial antenna link and displayed on the ground control station for monitoring. To allow manual override from ground in the case of an emergency, a limited set of commands to control the experiment (e.g. change laser currents, switch between beam path configurations A, B and C, switch off lasers) was available.

3 Results

On 23rd of January 2016, the KALEXUS experiment was launched on-board the TEXUS 53 sounding rocket from the Esrange Swedish Space Center near Kiruna, Sweden. Both lasers could be stabilized in microgravity and the tests of redundancy concepts were successful. With the software for autonomous experiment control fully functioning, we did not use any manual experiment control throughout flight. The following sections firstly describe the experiment sequence and secondly the frequency stabilization during flight.

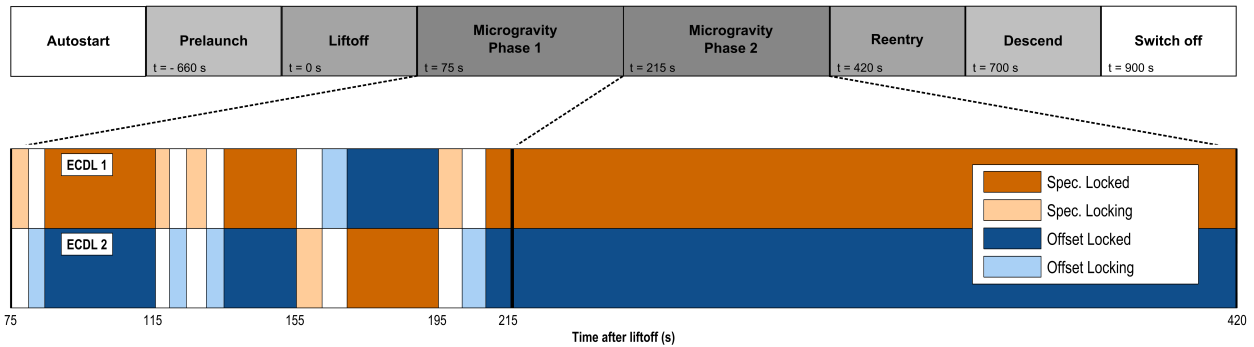


Fig. 6 Top: The different states of the experiment before and throughout the flight. Bottom: ECDL 1 and ECDL 2 in microgravity during flight. Here, each laser is in one of four modes: 1. Frequency locked on spectroscopy signal (dark orange), 2. Currently trying to spectroscopy lock (light orange), 3. Frequency locked on beat note frequency (dark blue), 4. Currently trying to offset lock (light blue). During microgravity, the different optical paths result in a swap of the laser function from spectroscopy lock to offset lock and vice versa, at $t = 155$ s and $t = 195$ s. White indicates that no locking information is accessible: during locking of one laser, the system is occupied and can not provide information about the other laser.

3.1 Flight

During the TEXUS 53 sounding rocket flight, the peak acceleration along the direction of flight (z -axis) reached $12.1 g$ during launch and up to $15.7 g$ along the other axes during reentry [39]. With a maximum altitude of 252.6 km, TEXUS 53 achieved 367 seconds of microgravity ($< 10^{-4} g$).

The timeline of the experiment sequence during flight is shown schematically in Figure 6 (top). As soon as the KALEXUS experiment was switched on, it initiated laser thermalization, frequency stabilization, monitoring and prepared the system to be ready for liftoff. Before launch, at $t = -660$ s, the prelaunch state started and data recording was activated. With liftoff at $t = 0$ s, vibrations set in during motor ignition and ascend flight. To protect our hardware, the state-machine was programmed to limit the experiment’s functionality during launch by disabling the optical switch. Microgravity was reached at $t = 73$ s and lasted until $t = 440$ s. Microgravity phases 1 and 2 were the main testing time, in which different experimental sequences were activated and redundancy and frequency stabilization tests were performed. Strong vibrations also occurred during reentry in the atmosphere from around $t = 460$ s, which ceased after parachute deployment at $t = 620$ s. From that point onwards, the payload slowly descended to the ground, where it landed at $t = 888$ s. The OBC recorded data from several minutes before liftoff until right after landing ($t = 900$ s), when the experiment received the signal to switch off.

3.2 Frequency stabilization during flight

Both lasers were switched on throughout the whole flight until the experiment was powered off, and we had automated frequency stabilization activated at all times. Due

to the vibrations during launch, the frequency stabilization was disturbed and had to be re-initiated by the locking state-machine. Several seconds after the vibrations subsided, both lasers could be stabilized. Here, we focus on describing the frequency stabilization in microgravity, after launch, since this will be the relevant experimental environment in future science missions. Results of the laser stabilization monitoring for the duration of microgravity are shown in the bottom part of Figure 6. ECDL 1 is shown in the top and ECDL 2 in the bottom part of the graph.

At $t = 75$ s, phase 1 of the KALEXUS experiment began, in which the automated frequency stabilization and redundancy hardware were tested. We implemented a mandatory re-initialization of the locking mechanism when microgravity set in, which is reflected in the data. At times $t_B = 115$ s, $t_C = 155$ s and $t_A = 195$ s, the state-machine received programmed signals to actively change the optical path and re-stabilize the lasers by initializing the stabilization algorithm. The spectroscopy stabilization was activated first, the offset stabilization followed afterward. At all three times, we observed successful stabilization of both lasers. In two cases, it took one attempt and in one case ($t_B = 115$ s) it took two attempts for successful stabilization. We recorded the respective saturated absorption error signals of ^{39}K on ground and during flight at three different times during microgravity (in all three optical path configurations), which are shown in Figure 7. The scan frequency is around 23 Hz. Also shown is a scan of the beat note signal that was used for offset locking. The spectra observed on ground and during flight agree qualitatively. Deviations in signal amplitude are due to differences in the optical power among the different paths. The small oscillations visible in the error signals recorded during flight have also been observed on ground and are most likely due to an etalon effect in the system, which is

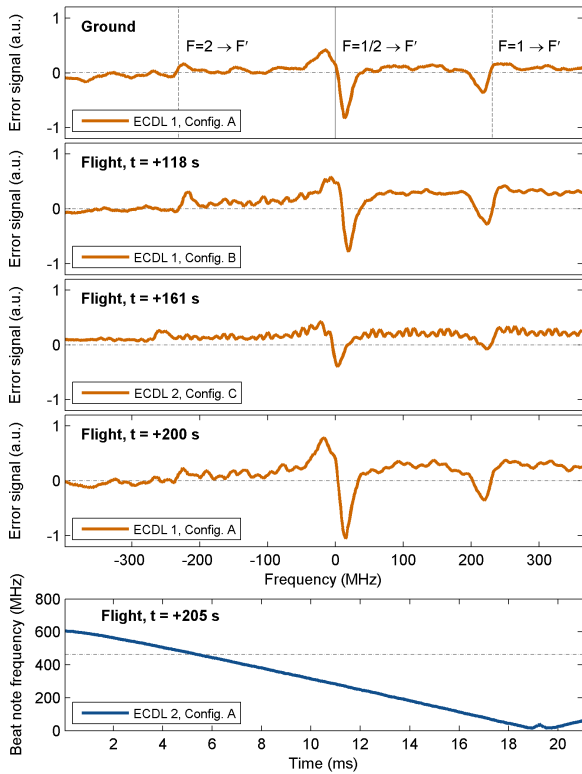


Fig. 7 Absorption spectroscopy error signal of ^{39}K on ground for optical path configuration A and during flight for all three configurations, A, B and C. The horizontal dashed lines indicate the lock points of the signal, i.e. the setpoint for the error signal feedback loop for the spectroscopy lock. D_2 transitions and crossover of ^{39}K are labeled. The bottom graph also shows a scan of the beat note signal that is used for offset locking, with the dashed line indicating the desired offset frequency (here: 464 MHz).

currently under investigation as part of the post-flight analysis.

Phase 2 of the KALEXUS experiment started at $t = 215$ s. During phase 2, both lasers were kept stabilized and parameters such as laser temperatures, laser currents, beat note frequency and error signal were monitored to test longer timescale behavior of the lasers and potential drifts. We did observe a constant increase in feedback current for the laser stabilization over time, which relates to an overall temperature increase of the hardware during flight. However, over the complete remaining microgravity duration of 225 s, we observed an uninterrupted spectroscopy lock of ECDL 1 and offset lock of ECDL 2. For additional monitoring, a beat note measurement was performed throughout the flight between ECDL 2 and an external frequency comb by Menlo Systems in a separate payload on the same rocket [29, 30]. This beat note measurement confirmed independently that both lasers were frequency stabilized during phase 2.

During reentry – as during launch – the high vibrations disturbed the frequency stabilization, and the

locking mechanism was engaged. After acceleration decreased, both lasers could be re-stabilized. The hardware survived the flight and was fully functioning after recovery.

4 Summary and Outlook

With the KALEXUS experiment, we have built a laser system technology demonstrator on a sounding rocket. Its core technologies are micro-integrated ECDLs, a spectroscopy board made of Zerodur, compact electronics, and an autonomously operating control software. The laser system was designed and built with future spaceborne setups for cold atom quantum sensors in mind. To demonstrate functionality in a space environment, KALEXUS was launched on-board the TEXUS 53 sounding rocket. During flight, all experimental sequences were performed autonomously. These included automatic frequency stabilization of two micro-integrated ECDLs at 766.7 nm with two different methods: one laser was frequency stabilized with an absorption spectroscopy signal of ^{39}K while the second laser was stabilized using the beat note frequency of the two lasers. Both lasers stayed frequency stabilized over the designated testing duration of 225 s in microgravity. In addition, hardware and software redundancy concepts were successfully tested during flight. The flight proven system thus achieved a TRL of 9 for sounding rocket application, following the ESA classifications [22, 23].

With this level of technological maturity, we can aim to implement the KALEXUS technologies into more complex experimental setups, e.g. to push for a space-based EEP test. In this context, ECDL technology is now a flight-proven option for applications requiring narrow linewidth light sources, such as cold atom experiments similar to those described in [18, 19, 13]. The single and dual species interferometry experiments on sounding rockets that are currently in preparation [40, 41, 12] are therefore no longer restricted to using rocket qualified DFB lasers [29, 30, 12]. Science missions on satellites, such as the proposed STE-QUEST [11], require a qualification of the KALEXUS technology beyond sounding-rockets [42, 23]. Additional environmental tests necessary for satellite-based science missions include exposure to radiation and thermal variations. These in combination with ongoing parallel technological developments for small satellites [43] and ISS-based experiments with cold atoms [7, 8, 44] will increase the available hardware for atomic physics and quantum optics experiments in space. As part of these developments, the sounding rocket qualification of the laser system technology achieved with the KALEXUS experiment was an important step towards application in space-based quantum sensors and beyond.

This work is supported by the German Space Agency DLR with funds provided by the Federal Ministry for Economic Affairs and Energy under grant number DLR 50WM1345.

We would like to thank C. Grzeschik for helpful discussions, M. Mihm for support with the integration of the optical system and Prof. Klaus Sengstock for providing the facilities for Zerodur technology integration at the Universität Hamburg. We would also like to thank Airbus DS for technical support throughout the mission, as well as SSC, MORABA and OHB for assistance during the launch campaign.

References

1. B. Schlepp, R. Kahle, J. Salepicco, S. Kuhlmann, and U. Sterr, “Laser communication with alphasat - FD challenges and first flight results,” 2014. 24th International Symposium on Space Flight Dynamics (ISSFD).
2. L. Cacciapuoti and C. Salomon, “Space clocks and fundamental tests: The ACES experiment,” *The European Physical Journal Special Topics*, vol. 172, no. 1, pp. 57–68, 2009.
3. J. D. Prestage and G. L. Weaver, “Atomic clocks and oscillators for deep-space navigation and radio science,” *Proceedings of the IEEE*, vol. 95, pp. 2235–2247, Nov 2007.
4. N. Yu, J. Kohel, J. Kellogg, and L. Maleki, “Development of an atom-interferometer gravity gradiometer for gravity measurement from space,” *Applied Physics B*, vol. 84, no. 4, pp. 647–652, 2006.
5. C. W. Chou, D. B. Hume, T. Rosenband, and D. J. Wineland, “Optical clocks and relativity,” *Science*, vol. 329, no. 5999, pp. 1630–1633, 2010.
6. O. Carraz, C. Siemes, L. Massotti, R. Haagmans, and P. Silvestrin, “A spaceborne gravity gradiometer concept based on cold atom interferometers for measuring earth’s gravity field,” *Microgravity Science and Technology*, vol. 26, no. 3, pp. 139–145, 2014.
7. T. Lévêque, L. Antoni-Micollier, B. Faure, and J. Berthon, “A laser setup for rubidium cooling dedicated to space applications,” *Applied Physics B*, vol. 116, no. 4, pp. 997–1004, 2014.
8. T. Lvque, B. Faure, F. X. Esnault, C. Delaroche, D. Massonnet, O. Grosjean, F. Buffe, P. Torresi, T. Bommer, A. Pichon, P. Braud, J. P. Lelay, S. Thomin, and P. Laurent, “PHARAO laser source flight model: Design and performances,” *Review of Scientific Instruments*, vol. 86, no. 3, 2015.
9. J. M. Hogan, D. M. S. Johnson, S. Dickerson, T. Kovachy, A. Sugarbaker, S.-w. Chiow, P. W. Graham, M. A. Kasevich, B. Saif, S. Rajendran, P. Bouyer, B. D. Seery, L. Feinberg, and R. Keski-Kuha, “An atomic gravitational wave interferometric sensor in low earth orbit (AGIS-LEO),” *General Relativity and Gravitation*, vol. 43, no. 7, pp. 1953–2009, 2011.
10. P. W. Graham, J. M. Hogan, M. A. Kasevich, and S. Rajendran, “New method for gravitational wave detection with atomic sensors,” *Physical Review Letters*, vol. 110, p. 171102, Apr 2013.
11. D. N. Aguilera, H. Ahlers, B. Battelier, A. Bawamia, A. Bertoldi, R. Bondarescu, K. Bongs, P. Bouyer, C. Braxmaier, L. Cacciapuoti, C. Chaloner, M. Chwalla, W. Ertmer, M. Franz, N. Gaaloul, M. Gehler, D. Gerardi, L. Gesa, N. Gürlebeck, J. Hartwig, M. Hauth, O. Hellmig, W. Herr, S. Herrmann, A. Heske, A. Hinton, P. Ireland, P. Jetzer, U. Johann, M. Krutzik, A. Kubelka, C. Lämmerzahl, A. Landragin, I. Lloro, D. Massonnet, I. Mateos, A. Milke, M. Nofrarias, M. Oswald, A. Peters, K. Posso-Trujillo, E. Rasel, E. Rocco, A. Roura, J. Rudolph, W. Schleich, C. Schubert, T. Schuldt, S. Seidel, K. Sengstock, C. F. Sopauerta, F. Sorrentino, D. Summers, G. M. Tino, C. Trenkel, N. Uzunoglu, W. von Klitzing, R. Walser, T. Wendrich, A. Wenzlawski, P. Weßels, A. Wicht, E. Wille, M. Williams, P. Windpassinger, and N. Zahzam, “STE-QUEST – test of the universality of free fall using cold atom interferometry,” *Classical and Quantum Gravity*, vol. 31, no. 11, p. 115010, 2014.
12. V. Schkolnik, O. Hellmig, A. Wenzlawski, J. Grosse, A. Kohfeldt, K. Döringshoff, A. Wicht, P. Windpassinger, K. Sengstock, C. Braxmaier, M. Krutzik, and A. Peters, “A compact and robust diode laser system for atom interferometry on a sounding rocket,” *Applied Physics B*, vol. 122, no. 8, pp. 1–8, 2016.
13. D. Schlippert, J. Hartwig, H. Albers, L. L. Richardson, C. Schubert, A. Roura, W. P. Schleich, W. Ertmer, and E. M. Rasel, “Quantum Test of the Universality of Free Fall,” *Physical Review Letters*, vol. 112, p. 203002, May 2014.
14. L. Zhou, S. Long, B. Tang, X. Chen, F. Gao, W. Peng, W. Duan, J. Zhong, Z. Xiong, J. Wang, Y. Zhang, and M. Zhan, “Test of equivalence principle at 10^{-8} level by a dual-species double-diffraction raman atom interferometer,” *Physical Review Letters*, vol. 115, p. 013004, Jul 2015.
15. P. Bouyer, G. Varoquaux, R. Nyman, and J.-P. Brantut, “ICE : atom interferometry in microgravity for testing the universality of free fall,” in *37th COSPAR Scientific Assembly*, vol. 37 of *COSPAR Meeting*, p. 364, 2008.
16. T. Schuldt, C. Schubert, M. Krutzik, L. G. Bote, N. Gaaloul, J. Hartwig, H. Ahlers, W. Herr, K. Posso-Trujillo, J. Rudolph, S. Seidel, T. Wendrich, W. Ertmer, S. Herrmann, A. Kubelka-Lange, A. Milke, B. Rievers, E. Rocco, A. Hinton, K. Bongs, M. Oswald, M. Franz, M. Hauth, A. Peters, A. Bawamia, A. Wicht, B. Battelier, A. Bertoldi, P. Bouyer, A. Landragin, D. Massonnet, T. Lévêque, A. Wenzlawski, O. Hellmig, P. Windpassinger, K. Sengstock, W. von Klitzing, C. Chaloner, D. Summers, P. Ireland, I. Mateos, C. F. Sopauerta, F. Sorrentino, G. M. Tino, M. Williams, C. Trenkel, D. Gerardi, M. Chwalla, J. Burkhardt, U. Johann, A. Heske, E. Wille, M. Gehler, L. Cacciapuoti, N. Gürlebeck, C. Braxmaier, and E. Rasel, “Design of a dual species atom interferometer for space,” *Experimental Astronomy*, vol. 39, pp. 167–206, June 2015.
17. T. van Zoest, N. Gaaloul, Y. Singh, H. Ahlers, W. Herr, S. T. Seidel, W. Ertmer, E. Rasel, M. Eckart, E. Kajari, S. Arnold, G. Nandi, W. P. Schleich, R. Walser, A. Vogel, K. Sengstock, K. Bongs, W. Lewoczko-Adamczyk, M. Schiemangk, T. Schuldt, A. Peters, T. Koenemann, H. Müntinga, C. Lämmerzahl, H. Dittus, T. Steinmetz, T. W. Hänsch, and J. Reichel, “Bose-Einstein Condensation in Microgravity,” *Science*, vol. 328, p. 1540, 2010.
18. S. Herrmann, H. Dittus, C. Lämmerzahl, and the QUANTUS and PRIMUS Teams, “Testing the equivalence

- principle with atomic interferometry,” Classical and Quantum Gravity, vol. 29, no. 18, p. 184003, 2012.
19. H. Müntinga, H. Ahlers, M. Krutzik, A. Wenzlawski, S. Arnold, D. Becker, K. Bongs, H. Dittus, H. Duncker, N. Gaaloul, C. Gherasim, E. Giese, C. Grzeschik, T. W. Hänsch, O. Hellmig, W. Herr, S. Herrmann, E. Kajari, S. Kleinert, C. Lämmerzahl, W. Lewoczko-Adamczyk, J. Malcolm, N. Meyer, R. Nolte, A. Peters, M. Popp, J. Reichel, A. Roura, J. Rudolph, M. Schiemangk, M. Schneider, S. T. Seidel, K. Sengstock, V. Tamma, T. Valenzuela, A. Vogel, R. Walser, T. Wendrich, P. Windpassinger, W. Zeller, T. van Zoest, W. Ertmer, W. P. Schleich, and E. M. Rasel, “Interferometry with bose-einstein condensates in microgravity,” Physical Review Letters, vol. 110, p. 093602, Feb 2013.
 20. E. Luvsandamdin, C. Kürbis, M. Schiemangk, A. Sahm, A. Wicht, A. Peters, G. Erbert, and G. Tränkle, “Micro-integrated extended cavity diode lasers for precision potassium spectroscopy in space,” Optics Express, vol. 22, pp. 7790–7798, Apr 2014.
 21. G. C. Bjorklund, “Frequency-modulation spectroscopy: a new method for measuring weak absorptions and dispersions,” Optics Letters, vol. 5, pp. 15–17, Jan 1980.
 22. ESA, “Technology readiness level.” <http://sci.esa.int/sci-ft/50124-technology-readiness-level/>. [Online; accessed 25-August-2016].
 23. ESA TEC-SHS, “Technology readiness level handbook for space applications.” https://artes.esa.int/sites/default/files/TRL_Handbook.pdf, 2008. [Online; accessed 25-August-2016].
 24. DLR, “TEXUS - mit forschungsraketen in die schwerelosigkeit - sounding rockets for microgravity research.” http://www.dlr.de/rd/Portaldata/28/Resources/dokumente/publikationen/Broschuere_TEXUS_hires.pdf. [Online; accessed 27-October-2016].
 25. ESA, “User guide to low gravity platforms, chapter 6 - sounding rockets.” <http://wsn.spaceflight.esa.int/docs/EUG2LGPPr3/EUG2LGPPr3-6-SoundingRockets.pdf>. [Online; accessed 27-October-2016].
 26. B. Franke, “Program description and user scenario - TEXUS / MAXUS / MINITEXUS,” in Microgravity Research and Applications in Physical Sciences and Biotechnology (O. Minster and B. Schürmann, eds.), vol. 454 of ESA Special Publication, p. 935, 2001.
 27. A. F. Palmerio, E. D. Roda, P. Turner, and W. Jung, “Results from the first flight of the VSB-30 sounding rocket,” in 17th ESA Symposium on European Rocket and Balloon Programmes and Related Research (B. Warmbein, ed.), vol. 590 of ESA Special Publication, pp. 345–349, Aug. 2005.
 28. A. Garcia, S. S. C. Yamanaka, A. N. Barbosa, F. C. P. Bizarria, W. Jung, and F. Scheuerpflug, “VSB-30 sounding rocket: history of flight performance,” Journal of Aerospace Technology and Management, vol. Vol.3, pp. 325–330, September 2011.
 29. M. Lezius, T. Wilken, C. Deutsch, M. Giunta, O. Mandel, A. Thaller, V. Schkolnik, M. Schiemangk, A. Dinkelaker, M. Krutzik, A. Kohfeldt, A. Wicht, A. Peters, O. Hellmig, H. Duncker, K. Sengstock, P. Windpassinger, K. Lampmann, T. Hülsing, T. W. Hänsch, and R. Holzwarth, “Space-born frequency comb metrology,” Optica, accepted for publication.
 30. M. Giunta, M. Lezius, C. Deutsch, T. Wilken, T. W. Hänsch, A. Kohfeldt, A. Wicht, V. Schkolnik, M. Krutzik, H. Duncker, O. Hellmig, K. Lampmann, A. Wenzlawski, P. Windpassinger, K. Sengstock, A. Peters, and R. Holzwarth, “Optical frequency combs for space applications,” in Conference on Lasers and Electro-Optics, p. STh4H.5, Optical Society of America, 2016.
 31. M. Schmidt, M. Prevedelli, A. Giorgini, G. M. Tino, and A. Peters, “A portable laser system for high-precision atom interferometry experiments,” Applied Physics B, vol. 102, no. 1, pp. 11–18, 2011.
 32. J. Le Gouët, P. Cheinet, J. Kim, D. Holleville, A. Clairon, A. Landragin, and F. Pereira Dos Santos, “Influence of lasers propagation delay on the sensitivity of atom interferometers,” The European Physical Journal D, vol. 44, no. 3, pp. 419–425, 2007.
 33. M. Schiemangk, K. Lampmann, A. Dinkelaker, A. Kohfeldt, M. Krutzik, C. Kürbis, A. Sahm, S. Spießberger, A. Wicht, G. Erbert, G. Tränkle, and A. Peters, “High-power, micro-integrated diode laser modules at 767 and 780 nm for portable quantum gas experiments,” Applied Optics, vol. 54, pp. 5332–5338, Jun 2015.
 34. W. Lewoczko-Adamczyk, C. Pyrlík, J. Häger, S. Schwertfeger, A. Wicht, A. Peters, G. Erbert, and G. Tränkle, “Ultra-narrow linewidth DFB-laser with optical feedback from a monolithic confocal fabry-perot cavity,” Optics Express, vol. 23, pp. 9705–9709, Apr 2015.
 35. Schott AG, “ZERODUR® Extremely Low Expansion Glass Ceramic.” http://www.schott.com/advanced_optics/english/syn/advanced_optics/products/optical-materials/zerodur-extremely-low-expansion-glass-ceramic/zerodur/index.html. [Online; accessed 25-August-2016].
 36. H. Duncker, O. Hellmig, A. Wenzlawski, A. Grote, A. J. Rafipoor, M. Rafipoor, K. Sengstock, and P. Windpassinger, “Ultrastable, zerodur-based optical benches for quantum gas experiments,” Applied Optics, vol. 53, pp. 4468–4474, Jul 2014.
 37. All cards for experiment control have been developed by Leibniz-Universität Hannover for previous laser control and cold atom experiments, but were adjusted to match the required specifications of the KALEXUS experiment.
 38. W. Bartosch, “Automatic frequency lock of a diode laser for rubidium spectroscopy.” Bachelor thesis, 2013. Gottfried Wilhelm Leibniz Universität Hannover.
 39. Quicklook TEXUS 53. Data provided by OHB SE (2016).
 40. T. van Zoest, A. Peters, H. Ahlers, A. Wicht, A. Vogel, A. Wenzlawski, C. Deutsch, E. Kajari, N. Gaaloul, H. Dittus, J. Hartwig, W. Herr, S. Herrmann, J. Reichel, K. Bongs, T. Koenemann, C. Laemmerzahl, W. Lewoczko-Adamczyk, M. Schiemangk, H. Müntinga, N. Meyer, E. M. Rasel, R. Walser, A. Resch, C. Rode, S. Seidel, K. Sengstock, Y. Singh, W. Schleich, W. Ertmer, P. Rosenbusch, T. Wilken, and E. Goeklue, “Towards a matter wave interferometer on a sounding rocket,” in 38th COSPAR Scientific Assembly, vol. 38 of COSPAR Meeting, p. 2, 2010.
 41. A. Stamminger, J. Ettl, J. Grosse, M. Hörschgen-Eggers, W. Jung, A. Kallenbach, G. Raith, W. Saedtler, S. Seidel, J. Turner, and M. Wittkamp, “MAIUS-1 - vehicle, subsystems design and mission operations,” in

22nd ESA Symposium on European Rocket and Balloon Programmes and Related Research, vol. SP-730, pp. 183–190, ESA Communications, September 2015.

42. STE-QUEST Study Team, “STE-QUEST mission requirements document.” <http://sci.esa.int/ste-quest/50187-ste-quest-mission-requirements-document/>, 2012. [Online; accessed 25-August-2016].
43. D. K. L. Oi, A. Ling, J. A. Grieve, T. Jennewein, A. N. Dinkelaker, and M. Krutzik, “Nanosatellites for quantum science and technology,” Contemporary Physics, accepted for publication.
44. NASA JPL, “CAL cold atom laboratory - mission overview.” <http://coldatomlab.jpl.nasa.gov/mission/>. [Online; accessed 25-August-2016].